

# A new fine-tuning problem in standard model: quantum chromodynamics trilemma

Chuan-Xin Cui,<sup>1,\*</sup> Jin-Yang Li,<sup>1,†</sup> Shinya Matsuzaki,<sup>1,‡</sup> Mamiya Kawaguchi,<sup>2,§</sup> and Akio Tomiya<sup>3,¶</sup>

<sup>1</sup>Center for Theoretical Physics and College of Physics, Jilin University, Changchun, 130012, China

<sup>2</sup>Department of Physics and Center for Field Theory and Particle Physics, Fudan University, 220 Handan Road, 200433 Shanghai, China

<sup>3</sup>RIKEN BNL Research center, Brookhaven National Laboratory, Upton, NY, 11973, USA

We find that a serious fine-tuning exists in quantum chromodynamics (QCD) at physical point, which involves three fundamental quantities essential for the QCD vacuum structure: susceptibility functions for the chiral symmetry, axial symmetry, and the topological charge. The fine-tuning is unavoidably driven when the balance in magnitude among them (dubbed the QCD trilemma) is relaxed. It turns out that QCD is actually “unnatural” at vacuum, and even in a whole low-temperature regime including the chiral crossover epoch. It may be challenging to resolve this “unnaturalness” in a whole thermal history of Universe even going beyond the framework of the standard model, because it is tightly tagged with the anomalous Ward identity for chiral and axial symmetries of the up, down and strange quarks. A supercooling first-order electroweak phase-transition might be one possibility to realize the “naturalness” at higher temperatures.

Several fine-tuning issues have been pointed out in the fields of particle physics and cosmology. In the standard model of particle physics, there are well-known two longstanding fine-tuning problems: one is related to the gauge hierarchy problem [1–4], while the other is the so-called strong CP problem in QCD [5–7]. The most gigantic tuning is required in cosmology, to account for the presently accelerating Universe, so-called the cosmological constant problem [8]. Taking them seriously into account has so far motivated us to refine or go beyond the existing theories, the standard model and Einstein general relativity, and opened numerous frontiers in research directions along the theoretical particle and cosmological physics.

In this Letter, we pose a new fine-tuning problem in the thermal history of the standard model. We find that a serious fine-tuning potentially exists in three fundamental quantities essential to characterize the vacuum structure of QCD: susceptibility functions for the chiral  $SU(2)_L \times SU(2)_R$  symmetry, the  $U(1)_A$  axial symmetry, and the topological susceptibility.

Those three susceptibilities are robustly related to each other by the anomalous Ward identities for the chiral  $SU(3)_L \times SU(3)_R$  symmetry, to hold the form symbolically like

$$\langle \text{Chiral } SU(2) \rangle = \langle U(1) \text{ Axial} \rangle - \langle \text{Topological} \rangle, \quad (1)$$

where brackets stand for vacuum expectation values or thermally averaged amplitudes. For the precise expressions written in terms of the susceptibilities, see Eq.(3).  $\langle \text{Chiral } SU(2) \rangle$  or  $\langle U(1) \text{ Axial} \rangle$  goes to zero, when the chiral  $SU(2)_L \times SU(2)_R$  symmetry or  $U(1)_A$  symmetry

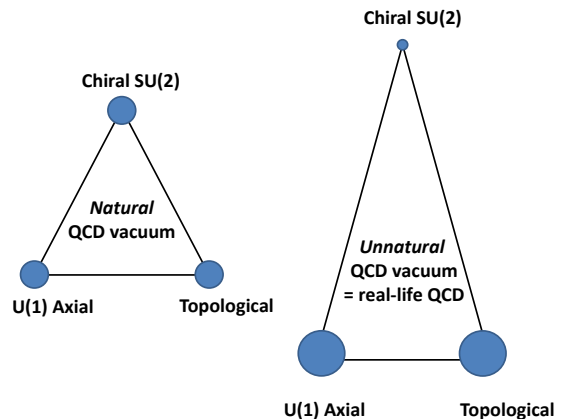


FIG. 1: Illustration of QCD trilemma and its relaxation. The QCD vacuum structure is built upon the “Chiral  $SU(2)$ ”, “ $U(1)$  Axial”, and “Topological” features, which are related each other by a balance relation like Eq.(1) (or, more precisely given in Eq.(3)). Left panel: the theory is *natural* and holds the trilemma by forming the equilateral triangle with the same order of the weight amplitudes denoted by blobs. Right panel: the trilemma is violated (relaxed) when a fine-tuning is caused by a big cancellation between “ $U(1)$  Axial”, and “Topological” in Eq.(1), which is represented by the isosceles triangle with one blob significantly reduced, keeping Eq.(1) and the corresponding two sides stretched out. Hence the theory is *unnatural*, that turns out to be the case of real-life QCD (the relaxation pattern (i) in Eq.(2)), as is demonstrated in the text.

is restored. One might simply think that the above three amplitudes should take the same order of magnitude, namely, no preference among them in magnitude, so that the Ward identity acts like a balance equation. This case is thought to be *natural*, where no fine-tuning is present. We do this as “trilemma”, and depict a triangle cartoon in Fig. 1.

The trilemma will be violated when one of three amplitudes gets drastically smaller than others; e.g. it is the

\*cuicx1618@mails.jlu.edu.cn

†lijy1118@mails.jlu.edu.cn

‡synya@jlu.edu.cn

§kawaguchi@fudan.edu.cn

¶akio.tomiya@riken.jp

$$\chi_\pi \xleftrightarrow{\text{U(1) Axial}} \chi_\delta \xleftrightarrow{\text{Chiral SU(2)}} \chi_\eta$$

FIG. 2: Relations for the chiral and axial susceptibilities

case when

$$\begin{aligned} \text{(i)} \quad & \frac{\langle \text{Chiral SU(2)} \rangle}{\langle \text{U(1) Axial} \rangle} = 1 - \frac{\langle \text{Topological} \rangle}{\langle \text{U(1) Axial} \rangle} \ll 1; \\ \text{(ii)} \quad & \frac{\langle \text{Topological} \rangle}{\langle \text{U(1) Axial} \rangle} = 1 - \frac{\langle \text{Chiral SU(2)} \rangle}{\langle \text{U(1) Axial} \rangle} \ll 1. \end{aligned} \quad (2)$$

In the case (i), when the chiral symmetry is restored,  $\langle \text{Chiral SU(2)} \rangle$  is finely tuned to zero by  $\langle \text{U(1) Axial} \rangle$  and  $\langle \text{Topological} \rangle$ , while the case (ii) the tuned amplitude is  $\langle \text{Topological} \rangle$  by a gigantic cancellation between  $\langle \text{Chiral SU(2)} \rangle$  and  $\langle \text{U(1) Axial} \rangle$ . This is thus *unnatural*, as illustrated in the right panel of Fig. 1.

We find that QCD is actually *unnatural* in a sense of the trilemma relaxation pattern (i) in Eq.(2), i.e., due to the fine-tuned chiral order parameter. It is demonstrated based on a chiral effective theory that the *unnaturalness* stays in a whole low-temperature regime including the chiral phase transition (crossover). The size of the tuning is found to be two orders of magnitude even at vacuum:  $R \equiv 1 - \frac{\langle \text{Topological} \rangle}{\langle \text{U(1) Axial} \rangle} = \mathcal{O}(10^{-2})$ , and this  $R$  is to be somewhat smaller at around the chiral crossover, which turns out to be actually in good agreement with the reported lattice result.

We conjecture that the *unnaturalness* of QCD is related to the flavor violation in three-flavor quark masses, which is dictated to be sizable today, and shown to keep sizable even still around the chiral crossover epoch.

To see how the chance of the chiral symmetry restoration is potentially *unnatural*, we start with a relation between order parameters for the chiral  $SU(2)_L \times SU(2)_R$  symmetry and  $U(1)_A$  axial symmetry, which is constructed from a set of generic anomalous Ward identities for the three-flavor chiral  $SU(3)_L \times SU(3)_R$  symmetry. The relation goes like

$$\chi_{\eta-\delta} = \chi_{\pi-\delta} + \frac{4}{m_l^2} \chi_{\text{top}}, \quad (3)$$

where  $m_l = m_u = m_d$  (isospin symmetric limit);  $\chi_{\eta-\delta} \equiv \chi_\eta - \chi_\delta$  and  $\chi_{\pi-\delta} \equiv \chi_\pi - \chi_\delta$  are differences of chiral and axial susceptibilities, which signal the restorations when those (asymptotically) reach zero;  $\chi_{\text{top}}$  is the topological susceptibility. The chiral and axial correlations for the  $\chi_{\eta-\delta}$  and  $\chi_{\pi-\delta}$  are summarized in Fig. 2. Note that those susceptibilities involve strange quark contributions at the loop level, hence depend on the strange quark mass  $m_s$ . More details on the susceptibilities are presented in Appendix A. Equation (3) is the precise form holding the QCD trilemma, symbolically described in Eq.(1):  $\chi_{\eta-\delta} \equiv \langle \text{Chiral SU(2)} \rangle$ ,  $\chi_{\pi-\delta} \equiv \langle \text{U(1) Axial} \rangle$ , and  $\chi_{\text{top}} \equiv \langle \text{Topological} \rangle$ . (Note  $\chi_{\text{top}} < 0$  and other

susceptibilities are positive in our sign convention. See also Appendix A.) Thus the QCD trilemma in Eq.(3) dictates the chiral  $SU(2)$  symmetry breaking and  $U(1)_A$  breaking, linked with the transition rate of the topological charge, where all the breaking is dominantly controlled by nonzero quark masses.

To facilitate the later discussion, we define a ratio

$$R \equiv \frac{\frac{4}{m_l^2} \chi_{\text{top}} + \chi_{\pi-\delta}}{\chi_{\eta-\delta} - \frac{4}{m_l^2} \chi_{\text{top}}} = 1 + \frac{\frac{4}{m_l^2} \chi_{\text{top}}}{\chi_{\pi-\delta}}. \quad (4)$$

By using this  $R$  the Ward identity in Eq.(3) is evaluated as

$$\chi_{\eta-\delta} = R \cdot \chi_{\pi-\delta}, \quad (5)$$

so that the ratio  $R$  measures the size of gap in magnitude between the chiral ( $\chi_{\eta-\delta}$ ) and axial ( $\chi_{\pi-\delta}$ ) susceptibilities.

When both susceptibilities asymptotically approach zero (i.e. get close to the restoration), a small  $R$ , e.g. less than  $\mathcal{O}(10\%)$ , parameterizes somewhat a serious fine-tuning by that amount: that is like  $R \sim 1 - (1 - \epsilon)$  with  $\epsilon = \mathcal{O}(10\%)$ . (Here the second term  $(\chi_{\text{top}}/\chi_{\pi-\delta}) < 0$  in our sign convention.) This corresponds to the case (i) in Eq.(2) for the trilemma relaxation. In addition, when  $R \rightarrow 1$  (say, 0.9),  $\chi_{\text{top}}$  is instead tuned to zero by another subtraction  $(\chi_{\eta-\delta} - \chi_{\pi-\delta})$ <sup>1</sup>. This is the case (ii) in Eq.(2). Thus, one may quantify the *naturalness* to keep the QCD trilemma, by saying that a theory is *natural* when

$$0.1 < R < 0.9, \quad \text{and} \quad R = 0, 1, \quad (6)$$

otherwise *unnatural* due to the accidental relaxation. When  $R$  is exactly equal to 1, the axial anomaly is absent, where obviously no fine tuning is seen, while in the case of  $R = 0$ , no chiral symmetry breaking is present, so is *natural*. We shall dub  $R$  as the trilemma-relaxation estimator.

The state-of-the-art lattice QCD simulations have revealed a faster dumping of  $\chi_{\eta-\delta}$ , than  $\chi_{\pi-\delta}$  around and above the chiral crossover temperature [11, 12], which indicates  $R \ll 1$  in Eq.(5). This is also supported from a rigorous argument based on QCD-inequality like relations [13] and its generalized evidence based on the lattice QCD setup [14]. Furthermore, a recent lattice study (with two lightest flavors) has shown significantly dominant contributions from the axial susceptibilities ( $\chi_{\pi-\delta}$  and  $\chi_{\text{top}}$ ) left in the chiral susceptibility ( $\chi_{\eta-\delta}$ ) in the chiral crossover domain [15]. This implies that there may be a fine-tuning to realize the faster-dumped and smaller

<sup>1</sup> This vanishing  $\chi_{\text{top}}$  happens due to the flavor-singlet nature [7, 16–18], which keeps operative even at finite temperature [16, 18]. Note also that this  $R \rightarrow 1$  corresponds to yielding a small value of the ratio (say 0.1 for  $R = 0.9$ ) in the case (ii) in Eq.(2).

$\chi_{\eta-\delta}$  by the destructive interference between more slowly dumped and larger  $\chi_{\pi-\delta}$  and  $\chi_{\text{top}}$ : i.e.  $R \ll 1$ , in Eq.(5). Thus, QCD seems to be *unnatural* in realizing the asymptotic-chiral symmetry restoration. Actually, though not explicitly addressed, this fine-tuning could be read off from the existing lattice QCD data [11] and also [15] with taking into account possible finite volume effects and statistical errors.

Prior to the lattice simulations, based on a chiral effective theory we demonstrate that it is indeed the case in a whole low-temperature regime including around the chiral crossover, and conjecture that it is due to the three-flavor symmetry violation.

We employ a Nambu-Jona-Lasinio (NJL) model with three flavors. In addition to the standard-scalar four-fermion interaction terms the model includes a determinant term (Kobayashi-Maskawa-'t Hooft [19–22]) which would be induced from the QCD instanton coupled to quarks and explicitly breaks the  $U(1)_A$  axial symmetry<sup>2</sup>. We refer readers to a review paper [23] and Appendix A as the details on the Lagrangian, the formalism at finite temperature, and the formulae of the chiral and axial susceptibilities. We adopt the same inputs as in the literature, working in the isospin symmetric limit ( $m_u = m_d = m_l$ ), to fix the model parameters at zero temperature ( $T = 0$ ). QCD at the physical point that we call real-life QCD, presently modeled by the NJL description, predicts  $m_l = 5.5$  MeV and  $m_s = 138$  MeV [23], which well reproduces the hadronic observables (pion decay constant, pion, kaon and eta prime masses, and so forth).

We have also found that the value of  $\chi_{\text{top}}$  at  $T = 0$  estimated from the present model is in good agreement with the lattice result, and the (subtracted and normalized) chiral condensate as well as the (normalized)  $\chi_{\text{top}}$  exhibit perfectly consistent  $T/T_{\text{pc}}$ -scalings in a qualitative sense, including below and above the chiral crossover point with the pseudo-critical temperature  $T_{\text{pc}|_{\text{NJL}}} \simeq 188$  MeV, in comparison with the lattice data. For the details, see Appendix A. This confirms that the present NJL model describes the chiral crossover phenomenon in real-life QCD quite well.

Figure 3 shows values of the trilemma-relaxation estimator  $R$  evolved with  $T$ , allowing  $m_s$  off the physical point with  $m_l$  kept physical. See the middle-solid curve with  $m_s = 138$  MeV, which corresponds to real-life QCD. Comparison with the available 2 + 1 flavor-lattice QCD

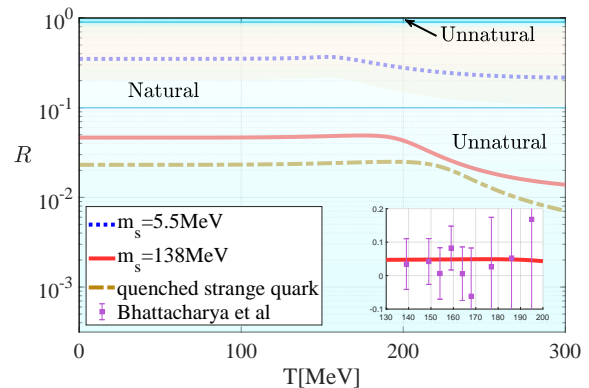


FIG. 3: Plots showing that real-life QCD is *unnatural* and conjecturing that the *naturalness* is recovered in the three-flavor symmetric limit, which are monitored by the trilemma-relaxation estimator  $R$  defined in Eq.(4). Estimates have been done based on the NJL model described as in the text. Comparison with the 2+1 flavor-lattice QCD data (with  $m_\pi = 135$  MeV) in the available  $T$  range has also been displayed with the error bars [11] (in the zoomed-in window). The curve with  $m_s = 138$  MeV points to real-life QCD with three flavors, while the quenched-strange quark limit has been achieved by taking  $m_s = 50$  GeV, corresponding to the two-flavor limit. Another curve with  $m_s = 5.5$  MeV denotes a conjectured prediction in the three-flavor symmetric limit. The *Natural* and *Unnatural* regimes are defined in Eq.(6).

data (with  $m_\pi = 135$  MeV) on  $R$  [11] — reconstructed from the data on  $\chi_{\pi-\delta}$  and  $\chi_{\eta-\delta}$  through the relation Eq.(5) — has also been displayed (in the zoomed-in window), which shows a good agreement including the error bars, for  $140 \text{ MeV} \lesssim T \lesssim 200 \text{ MeV}$ <sup>3</sup>.

Remarkably, in a whole low-temperature regime including the chiral crossover, real-life QCD stays outside the *Natural* region defined as in Eq.(6), required to have a sizable fine-tuning. We have observed  $R \simeq 0.05$  at around  $T$  covering the crossover point ( $T_{\text{pc}|_{\text{NJL}}} \simeq 188$  MeV:  $140 \text{ MeV} \lesssim T \lesssim 200 \text{ MeV}$ ), consistently with the lattice data, and  $R \lesssim 0.01$  at  $T \gtrsim 300$  MeV. Namely, the size of fine-tuning is slightly amplified by thermal loop effects as  $T$  develops from zero<sup>4</sup>.

Although the present model parameters are fixed at the physical point, we may deduce some conjectures on the *naturalness* in a view of the quark mass difference. Extrapolating off real-life QCD, one can then observe that the *Unnatural* domain still covers the two-flavor limit case

<sup>2</sup> We will not consider intrinsic-temperature dependent couplings, instead, all the  $T$  dependence should be induced only from the thermal quark loop corrections to the couplings defined and introduced at vacuum. Actually, the present NJL shows good agreement with lattice QCD results on the temperature scaling for the chiral, axial, and topological susceptibilities, as shown in Appendix B. In this sense, we do not need to introduce such an intrinsic  $T$  dependence for the model parameters in the regime up to temperatures around the chiral crossover.

<sup>3</sup> The individual  $\chi_{\pi-\delta}$  and  $\chi_{\eta-\delta}$  involve some discrepancy between the NJL estimate and the lattice data, on both of which the NJL tends to give larger values. For details, see Appendix B.

<sup>4</sup> Above  $T \sim 300$  MeV, the NJL description as the effective theory of QCD will be somewhat unreliable because the deconfining color degrees of freedom would be significant.

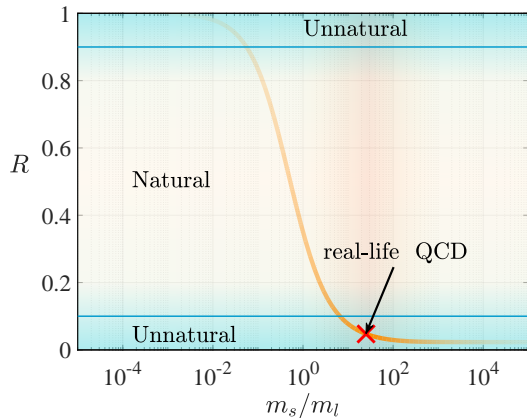


FIG. 4: Plots on the QCD trilemma-relaxation estimator  $R$  at  $T = 0$  as a function of  $m_s/m_l$ , along with the *Naturalness* interval defined in Eq.(6). The shaded domain surrounded by the real-life QCD point implies confidence level intervals for the model prediction, where the model parameters expect for  $m_s$  have been fixed at the physical point, as noted in the text. The thinner-shaded regions should be understood as indefinitely extrapolated results with somewhat poor reliability.

with  $m_s = 50$  GeV (bottom-dot-dashed curve), where strange quark is decoupled, and the required fine-tuning size is greater than that in the real-life QCD case. Taking the three-flavor symmetric limit  $m_s = m_l$  with  $m_l$  fixed to the physical value, we find a *Natural* QCD-like theory (top-dashed curve), which keeps almost constant  $R$  at any finite  $T$  within the *Naturalness* interval in Eq.(6). This implies that the three-flavor symmetry would be related to the relaxation of the QCD trilemma.

Since the order of magnitude for  $R$  tends to be almost fixed at  $T = 0$ , we may focus only on  $R$  at  $T = 0$ , and look into the flavor-symmetry dependence on  $R$ , by varying  $m_s$  in a wide range, with fixed  $m_l$  to the physical value. Figure 4 shows plots on  $R$  as a function of  $m_s/m_l$ , together with the *Naturalness* interval in Eq.(6). As  $m_s$  goes off the flavor symmetric limit in the *Natural* domain to be smaller,  $R$  tends to get larger, to flow into the *Unnatural* domain governed by the fine-tuning of  $\chi_{\text{top}}$  (that is the relaxation patten (ii) in Eq.(2)). The figure clearly shows that a *Natural* QCD-like theory should have had some approximate three-flavor symmetry for up, down and strange quarks with  $0.06 \lesssim m_s/m_l \lesssim 6$ .

In conclusion, real-life QCD is required to relax the trilemma associated with the essential feature of the vacuum structure of QCD, and inevitably is finely-tuned to reach the chiral symmetry restoration. This is schematically depicted in Fig. 1. Actually, this fine-tuning is present even at vacuum, which we conjectured is due to the three-flavor symmetry violation for up, down and strange quarks, and becomes more eminent after the chiral crossover. Those features can directly be tested on lattice QCD.

The discovered fine-tuning at  $T = 0$  (existing in  $R$ , in Eq.(5)) seems to be hard to be resolved in a simple-mind even if contributions beyond the standard model are taken into account, because the Ward-identity for the three-flavor chiral ( $SU(3)_L \times SU(3)_R$ ) in part includes the electroweak  $SU(2)$  gauge charge, to which light new physics contributions have severely been constrained by electroweak precision tests. Therefore, it would be inevitable to allow QCD to finely-tuned work for the chiral symmetry restoration and breaking at  $T = 0$  and also around the chiral crossover.

We have observed that an approximate three-flavor symmetry ( $m_l \sim m_s$ ) would make  $R$  *natural*. This implies that  $R$  can be kicked up into the *Natural* regime at higher  $T$  in the thermal history of Universe, where the three light quarks act as almost massless, hence the flavor symmetry can approximately work. Therefore, the fine-tuning problem might have been absent in some earlier epoch of the thermal history, which could not be covered by the framework of the present NJL model with  $T \lesssim 300$  MeV.

As  $T$  gets higher, the QCD instanton effects will be extremely diluted by an inverse Boltzman-like suppression  $\sim e^{-T^2/\mu_{\text{QCD}}^2}$  [25, 26] (with a collective scale factor of QCD,  $\mu_{\text{QCD}}$ ) as predicted from the dilute instanton gas description, so that the  $U(1)_A$ -breaking determinant term among quarks,  $\mathcal{L}_{\text{det}} = K \det(\bar{q}_L q_R) + \text{h.c.}$ , will also get significantly suppressed [24]. Actually,  $R \rightarrow$  larger as  $K \rightarrow$  smaller, because  $\chi_{\text{top}} \propto K$  and gets smaller (see Eq.(4)). Thereby one would suspect that  $R$  could jump in the *Natural* regime for  $0.1 < R < 0.9$ , above  $T \gtrsim 300$  MeV <sup>5</sup>.

To monitor  $R$  in such a higher- $T$  QCD, we may introduce a model having only  $\mathcal{L}_{\text{det}}$  plus the quark kinetic term, with the determinant coupling  $K$  simply scaled by temperature as  $K(T) = e^{-T^2/\mu_{\text{QCD}}^2} \cdot K$ . This determinant-type interaction would be of the most minimal form relevant to  $R$  dictating the chiral and axial breaking, which could mimic a “gluonic-interacting cloud” covering the quarks in quark-gluon plasma. More details on the model description and parameter setup for evaluation of  $R$  are provided in Appendix C. See Fig. 5, which indicates a possibility that  $R$  can be trapped in the *Unnatural* regime for  $0.9 < R < 1$  at  $T \sim 500 - 1000$  MeV. This takes place due to the highly suppressed  $K(T)$ , which promptly drives  $R$  up to close to 1 as  $T$

<sup>5</sup> As noted below Eq.(3), the QCD trilemma is controlled by the presence of the light three-flavor quark-masses, which would dominate the chiral and axial breaking effects, over other terms possibly arising from the (electromagnetic or electroweak) gauge interactions which explicitly break the global chiral  $SU(2)_L \times SU(2)_R$  symmetry. We have checked that those gauge interactions contribute as subleading terms arising at higher loop orders, so that this trend would keep operative unless the gauge interactions get nonperturbatively strong, which will not happen at least below the Planck scale.

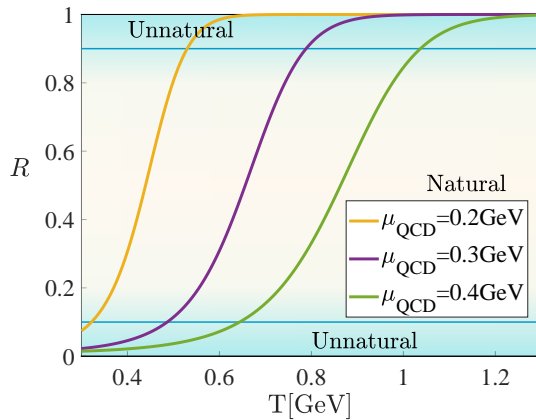


FIG. 5: Plots on a conjectured thermal evolution of  $R$  for a higher  $T$  regime up to around 1 GeV, based on a high- $T$  QCD model with three flavor quarks and the induced QCD instanton effect described in the text, more details of which are presented in Appendix C. The scale parameter  $\mu_{\text{QCD}}$  has been taken to be (200, 300, 400) MeV, as a reference.

gets higher. A decisive conclusion on  $R$  for  $T \gtrsim 300$  MeV can be derived from lattice QCD simulations with chiral fermions.

This unnaturalness again may be challenging to resolve even with new contributions beyond the standard model. One possible resolution could be a supercooling electroweak phase transition, such as addressed in the literature [27]. In this scenario, the quark mass  $m_l \rightarrow 0$  around the epoch of the chiral phase transition of QCD,

which makes  $R$  dropped down to  $R = 0$ , where in terms of Eq.(4)  $\frac{4\chi_{\text{top}}}{m_l^2}/\chi_{\pi-\delta}|_{m_l \rightarrow 0} \rightarrow -1$ , in which  $\chi_{\text{top}}|_{m_l \rightarrow 0} \rightarrow 0$ . Since this phase transition would be of the first order involving couplings of the standard model to new physics sector in a scale-invariant way,  $R$  could stay in the *Natural* regime.

We might also deduce some hints for beyond the standard models, even if the present-day-*unnaturalness* of relaxation of the QCD trilemma is not seriously taken into account: it would be led to a question on the origin of Yukawa coupling structures for the first-and second-generations quarks. The desired three-flavor symmetry might imply that the first-generation quarks can be thought of as somehow special, because of their separately small masses compared to the strange quark mass, or vice versa. This would support to consider the origin of Yukawa's with two separate and intrinsic scales, as what would be realized in warped extradimension models, some class of D-brane theories, or flavon models, and extended technicolor-like theories, and so forth.

#### Acknowledgement

We thank Tetsuo Hatsuda for giving us a crucial comment on the susceptibilities. This work was supported in part by the National Science Foundation of China (NSFC) under Grant No.11747308, 11975108, 12047569, and the Seeds Funding of Jilin University (S.M.). The work of A.T. was supported by the RIKEN Special Postdoctoral Researcher program and partially by JSPS KAKENHI Grant Number JP20K14479.

### Appendix A: The Nambu-Jona-Lasinio model

In this section, we give a brief introduction to the three-flavor Nambu-Jona-Lasinio (NJL) model as a low-energy chiral effective model of QCD. This model includes the 't Hooft determinant interaction term to incorporate the quantum  $U(1)_A$  anomaly, which would be induced from the QCD instanton, and the standard-scalar four fermion interaction term. Taking the auxiliary-field method to obtain meson spectra, the four-fermion and six-fermion interaction parts can be decomposed into various physical channels, by which scalar and pseudoscalar meson spectra can be well described. We will also give the susceptibility formulas for  $\pi$ ,  $\sigma$ ,  $\eta$  and  $\delta$  ( $= a_0$  in terms of the Particle Data Group) meson channels.

#### 1. Model description

The three flavor NJL model takes the form (for a review, see [23]):

$$\begin{aligned} \mathcal{L} &= \bar{q}(i\gamma_\mu \partial^\mu - \mathbf{m})q + \mathcal{L}_{4f} + \mathcal{L}_{\text{KMT}}, \\ \mathcal{L}_{4f} &= \frac{g_s}{2} \sum_{a=0}^8 [(\bar{q}\lambda^a q)^2 + (\bar{q}i\gamma_5 \lambda^a q)^2], \\ \mathcal{L}_{\text{KMT}} &= g_D [\det_{i,j} \bar{q}_i (1 + \gamma_5) q_j + \text{h.c.}], \end{aligned} \quad (\text{A1})$$

where the quark field  $q$  is represented as the triplet of  $SU(3)$ ,  $q = (u, d, s)^T$ , and  $\lambda^a$  ( $a = 0 \sim 8$ ) are the Gell-Mann matrices in the flavor space with  $\lambda^0 = \sqrt{2/3} \text{diag}(1, 1, 1)$ . The determinant in  $\mathcal{L}_{\text{KMT}}$  acts on the flavor indices and



the mass term  $\mathbf{m}$  is the current quark mass matrix,  $\mathbf{m} = \text{diag}(m_u, m_d, m_s)$ . In the following discussions, we assume the exact isospin symmetry  $m_u = m_d$  and define the light quark mass  $m_l = \frac{1}{2}(m_u + m_d)$ .

The  $\mathcal{L}_{4f}$  is the standard-scalar four fermion interaction term with the four-point coupling strength  $g_s$ . This is the most minimal interaction term involving the smallest number of quark fields for Lorentz scalar and pseudoscalar channels, which could be generated at low-energy QCD via the gluon exchange, and is  $U(3)_L \otimes U(3)_R$  invariant under the chiral transformation:  $q \rightarrow U \cdot q$  with  $U = \exp[-i\gamma_5 \sum_{a=0}^8 \lambda^a / 2\theta^a]$  and the chiral phases  $\theta^a$ . The mass term in  $\mathcal{L}$  explicitly breaks  $U(3)_L \otimes U(3)_R$  symmetry. The determinant term  $\mathcal{L}_{KMT}$  is called the Kobayashi- Maskawa-'t Hooft [19–22] term, which is a six-fermion interaction. This interaction gives rise to the mixing between different flavors and also uplift the  $\eta'$  mass to be no longer a Nambu-Goldstone (NG) boson. The KMT term preserves  $SU(3)_L \otimes SU(3)_R$  invariance (associated with the chiral phases labeled as  $a = 1, \dots, 8$ ) but breaks the  $U(1)_A$  (corresponding to  $a = 0$ ) symmetry, measured by the effective coupling constant  $g_D$ .

The NJL model itself is a (perturbatively) nonrenormalizable field theory because  $\mathcal{L}_{4f}$  and  $\mathcal{L}_{KMT}$  describe the higher dimensional interactions with mass dimension greater than four. Therefore, a momentum cutoff  $\Lambda$  must be introduced to make the NJL model regularized. All the parameters, including the cutoff  $\Lambda$ , will be fixed later in the numerical calculation section.

## 2. Quark condensate

At finite temperatures, the expectation value of an operator  $\Theta$  is given by the statistical thermal average:

$$\langle \Theta \rangle = \frac{\text{Tr} \Theta e^{-H/T}}{\text{Tr} e^{-H/T}}, \quad (\text{A2})$$

where  $H$  is the Hamiltonian operator.

We employ the mean-field approximation (MFA) and then obtain the gap equation and the thermodynamic potential. Then, the quark condensates acts as the parameters in the MFA and are  $T$ -dependent, which we define as

$$\langle \bar{u}u \rangle \equiv \alpha, \quad \langle \bar{d}d \rangle \equiv \beta, \quad \langle \bar{s}s \rangle \equiv \gamma. \quad (\text{A3})$$

Searching for the minimum point of the thermodynamic potential with respect to  $\alpha$ ,  $\beta$  and  $\gamma$  as variational parameters, the quark condensate formula are given as follows:

$$\langle \bar{q}_i q_i \rangle = -2N_c \int^\Lambda \frac{d^3p}{(2\pi)^3} \frac{M_i}{E_i} [1 - 2(\exp(E_i/T) + 1)^{-1}], \quad (\text{A4})$$

where  $E_i = \sqrt{M_i^2 + p^2}$ ,  $N_c$  denotes the number of colors to be fixed to three, and  $M_i$  are the dynamical masses:

$$\begin{aligned} M_u &= m_u - 2g_s\alpha - 2g_D\beta\gamma \\ M_d &= m_d - 2g_s\beta - 2g_D\alpha\gamma \\ M_s &= m_s - 2g_s\gamma - 2g_D\alpha\beta. \end{aligned} \quad (\text{A5})$$

## 3. Chiral and axial susceptibilities

In this subsection, we introduce susceptibilities for pseudoscalar and scalar meson channels and give their explicit formulas. We will leave the details of the calculations here and refer readers to a review paper [23], which contains all necessary information to reach the final formulas that we will present below.

### a. Pseudoscalar meson channel

In the  $\eta - \eta'$  coupled channel, the pseudoscalar meson susceptibility defined in the generator basis is defined as

$$\chi_P^{ij} = \int_T d^4x \langle (i\bar{q}(x)\gamma_5\lambda^i q(x))(i\bar{q}(0)\gamma_5\lambda^j q(0)) \rangle, \quad (\text{A6})$$

where  $i, j = 0, 8$  and  $\int_T d^4x \equiv \int_0^{1/T} d\tau \int d^3x$  with the imaginary time  $\tau = ix_0$ . This  $\chi_P^{ij}$  takes a matrix form

$$\chi_P = \frac{-1}{1 + G_P \Pi_P(0, 0)} \cdot \Pi_P(0, 0), \quad (\text{A7})$$

where  $G_P$  is the coupling strength matrix and  $\Pi_P$  is the polarization tensor matrix:

$$G_P = \begin{pmatrix} G_P^{00} & G_P^{08} \\ G_P^{80} & G_P^{88} \end{pmatrix} = \begin{pmatrix} g_s - \frac{2}{3}(\alpha + \beta + \gamma)g_D & -\frac{\sqrt{2}}{6}(2\gamma - \alpha - \beta)g_D \\ -\frac{\sqrt{2}}{6}(2\gamma - \alpha - \beta)g_D & g_s - \frac{1}{3}(\gamma - 2\alpha - 2\beta)g_D \end{pmatrix}, \quad (\text{A8})$$

$$\Pi_P = \begin{pmatrix} \Pi_P^{00} & \Pi_P^{08} \\ \Pi_P^{80} & \Pi_P^{88} \end{pmatrix} = \begin{pmatrix} \frac{2}{3}(2I_P^{uu} + I_P^{ss}) & \frac{2\sqrt{2}}{3}(I_P^{uu} - I_P^{ss}) \\ \frac{2\sqrt{2}}{3}(I_P^{uu} - I_P^{ss}) & \frac{2}{3}(I_P^{uu} + 2I_P^{ss}) \end{pmatrix}, \quad (\text{A9})$$

with  $I_P^{ii}(\omega, \mathbf{p})$  being the pseudoscalar one-loop polarization functions [28],

$$I_P^{ii}(0, 0) = -\frac{N_c}{\pi^2} \int_0^\Lambda dp p^2 \frac{1}{E_i} \left[ 1 - 2(\exp(M_i/T) + 1)^{-1} \right], \quad \text{for } i = u, d, s. \quad (\text{A10})$$

In our analyse, we mainly focus on susceptibility formulas in the flavor space, in which the pseudoscalar susceptibilities are defined by:

$$\begin{aligned} \chi_P^{l_1 l_2} &= \int_T d^4x \langle (i\bar{q}_{l_1}(0)\gamma_5 q_{l_1}(0))(i\bar{q}_{l_2}(x)\gamma_5 q_{l_2}(x)) \rangle, \quad \text{for } q_{l_{1,2}} = u, d, \\ \chi_P^{ss} &= \int_T d^4x \langle (i\bar{s}(0)\gamma_5 s(0))(i\bar{s}(x)\gamma_5 s(x)) \rangle, \\ \chi_P^{ls} &= \int_T d^4x \langle (i\bar{q}_l(0)\gamma_5 q_l(0))(i\bar{s}(x)\gamma_5 s(x)) \rangle, \quad \text{for } q_l = u, d. \end{aligned} \quad (\text{A11})$$

Then, by performing the basis transformation, the pseudoscalar susceptibilities in the flavor basis are obtained as

$$\begin{pmatrix} \frac{1}{2}\chi_P^{uu} + \frac{1}{2}\chi_P^{ud} \\ \chi_P^{us} \\ \chi_P^{ss} \end{pmatrix} = \begin{pmatrix} \frac{1}{6} & \frac{\sqrt{2}}{6} & \frac{1}{12} \\ \frac{1}{6} & -\frac{\sqrt{2}}{12} & -\frac{1}{6} \\ \frac{1}{6} & -\frac{\sqrt{2}}{3} & \frac{1}{3} \end{pmatrix} \begin{pmatrix} \chi_P^{00} \\ \chi_P^{08} \\ \chi_P^{88} \end{pmatrix}, \quad (\text{A12})$$

where we have taken the isospin symmetric limit into account, i.e.,  $\chi_P^{uu} = \chi_P^{dd}$  and  $\chi_P^{us} = \chi_P^{ds}$ .

In our analyse, we are particularly interested in the susceptibilities of  $\pi$  and  $\eta$  mesons in the pseudoscalar channel, because they are correlated with a set of chiral and  $U(1)_A$  transformations and are directly related with the topological susceptibility in QCD [29], which we will discuss in the later section.

The  $\eta$  meson susceptibility is defined as

$$\chi_\eta = \int_T d^4x \left[ \langle (i\bar{u}(0)\gamma_5 u(0))(i\bar{u}(x)\gamma_5 u(x)) \rangle + \langle (i\bar{d}(0)\gamma_5 d(0))(i\bar{d}(x)\gamma_5 d(x)) \rangle + 2\langle (i\bar{u}(0)\gamma_5 u(0))(i\bar{d}(x)\gamma_5 d(x)) \rangle \right]. \quad (\text{A13})$$

In the isospin symmetric limit,  $\chi_\eta$  can be given as

$$\chi_\eta = 2\chi_P^{uu} + 2\chi_P^{ud}. \quad (\text{A14})$$

The  $\pi$  meson susceptibility is defined as

$$\chi_\pi = \int_T d^4x \left[ \langle (i\bar{u}(0)\gamma_5 u(0))(i\bar{u}(x)\gamma_5 u(x)) \rangle_{\text{conn}} + \langle (i\bar{d}(0)\gamma_5 d(0))(i\bar{d}(x)\gamma_5 d(x)) \rangle_{\text{conn}} \right], \quad (\text{A15})$$

with  $\langle \dots \rangle_{\text{conn}}$  being the connected part of the correlation function. The explicit formula in the NJL model reads

$$\chi_\pi = \frac{-1}{1 + G_\pi \Pi_\pi(0, 0)} \cdot \Pi_\pi(0, 0), \quad (\text{A16})$$

where  $G_\pi = g_s + g_D\gamma$ , which is the coupling strength in the pion channel, and  $\Pi_\pi$  is the quark-loop polarization function for  $\chi_\pi$ , which is evaluated by using  $I_P^{ii}$  in Eq.(A10) as

$$\Pi_\pi = I_P^{uu} + I_P^{dd} = 2I_P^{uu}. \quad (\text{A17})$$

b. Scalar meson channel

The definitions of scalar susceptibilities are similar to those for pseudoscalars', which are given just by removing  $i\gamma_5$  in the definition of pseudoscalar susceptibilities, and supplying the appropriate one-loop polarization functions and the corresponding coupling constants.

In the 0 - 8 coupled channel, the scalar susceptibility matrix  $\chi_S$  is evaluated in the present NJL on the generator basis as

$$\chi_S = \frac{-1}{1 + G_S \Pi_S(0, 0)}, \quad (\text{A18})$$

where  $G_S$  is the coupling strength matrix,

$$G_S = \begin{pmatrix} G_S^{00} & G_S^{08} \\ G_S^{80} & G_S^{88} \end{pmatrix} = \begin{pmatrix} g_s + \frac{2}{3}(\alpha + \beta + \gamma)g_D & \frac{\sqrt{2}}{6}(2\gamma - \alpha - \beta)g_D \\ \frac{\sqrt{2}}{6}(2\gamma - \alpha - \beta)g_D & g_s + \frac{1}{3}(\gamma - 2\alpha - 2\beta)g_D \end{pmatrix}. \quad (\text{A19})$$

It is interesting to note that comparing the coupling constant matrices in the scalar and pseudoscalar channels (Eqs.(A8) and (A19)), the only difference is in the relative sign in front of  $g_D$ . This indicates the different role played by the  $U(1)_A$  anomaly in these two channels: attractive and repulsive interactions, respectively. The scalar polarization tensor matrix  $\Pi_S$  in Eq.(A18) is given by

$$\Pi_S = \begin{pmatrix} \Pi_S^{00} & \Pi_S^{08} \\ \Pi_S^{80} & \Pi_S^{88} \end{pmatrix} = \begin{pmatrix} \frac{2}{3}(2I_S^{uu} + I_S^{ss}) & \frac{2\sqrt{2}}{3}(I_S^{uu} - I_S^{ss}) \\ \frac{2\sqrt{2}}{3}(I_S^{uu} - I_S^{ss}) & \frac{2}{3}(I_S^{uu} + 2I_S^{ss}) \end{pmatrix}, \quad (\text{A20})$$

$$I_S^{ii}(0, 0) = -\frac{N_c}{\pi^2} \int_0^\Lambda p^2 dp \frac{E_{ip}^2 - M_i^2}{E_i^3} \{1 - 2[\exp(M_i/T) + 1]^{-1}\} \quad i = u, d, s. \quad (\text{A21})$$

By moving on to the flavor base via the base transformation, the scalar susceptibilities are cast into the form:

$$\begin{pmatrix} \frac{1}{2}\chi_S^{uu} + \frac{1}{2}\chi_S^{ud} \\ \chi_S^{us} \\ \chi_S^{ss} \end{pmatrix} = \begin{pmatrix} \frac{1}{6} & \frac{\sqrt{2}}{6} & \frac{1}{12} \\ \frac{1}{6} & -\frac{\sqrt{2}}{12} & -\frac{1}{6} \\ \frac{1}{6} & -\frac{\sqrt{2}}{3} & \frac{1}{3} \end{pmatrix} \begin{pmatrix} \chi_S^{00} \\ \chi_S^{08} \\ \chi_S^{88} \end{pmatrix}, \quad (\text{A22})$$

in which we have read  $\chi_S^{uu} = \chi_S^{dd}$  and  $\chi_S^{us} = \chi_S^{ds}$ .

In the scalar channel, we focus mainly on  $\sigma$  meson and  $\delta$  meson susceptibilities, which are chiral and  $U(1)_A$  partners of  $\eta$  and  $\pi$  mesons. These four susceptibilities will be our direct tools to monitor the restorations of chiral and  $U(1)_A$  symmetries later.

The  $\sigma$  meson susceptibility is defined as

$$\begin{aligned} \chi_\sigma &= \int_T d^4x [\langle (\bar{u}(0)u(0))(\bar{u}(x)u(x)) \rangle + \langle (\bar{d}(0)d(0))(\bar{d}(x)d(x)) \rangle + 2\langle (\bar{u}(0)u(0))(\bar{d}(x)d(x)) \rangle] \\ &= 2\chi_S^{uu} + 2\chi_S^{ud}. \end{aligned} \quad (\text{A23})$$

For the  $\delta$  meson susceptibility, it is defined as

$$\chi_\delta = \int_T d^4x [\langle (\bar{u}(0)u(0))(\bar{u}(x)u(x)) \rangle_{\text{conn}} + \langle (\bar{d}(0)d(0))(\bar{d}(x)d(x)) \rangle_{\text{conn}}]. \quad (\text{A24})$$

Similar to  $\chi_\pi$  in Eq.(A16), the explicit formula for  $\chi_\delta$  reads

$$\chi_\delta = \frac{-\Pi_\delta(0, 0)}{1 + G_\delta \Pi_\delta(0, 0)}, \quad (\text{A25})$$

where  $G_\delta = g_s - g_D\gamma$ , which is the coupling strength in the  $\delta$  channel, and  $\Pi_\delta = I_S^{uu} + I_S^{dd} = 2I_S^{uu}$  is the corresponding quark-loop polarization function.



#### 4. Topological susceptibility

The topological susceptibility  $\chi_{\text{top}}$  is related to the  $\theta$  vacuum configuration of QCD. It is defined as the curvature of the  $\theta$ -dependent vacuum energy  $V(\theta)$  in QCD at  $\theta = 0$ :

$$\chi_{\text{top}} = - \int_T d^4x \frac{\delta^2 V(\theta)}{\delta\theta(x)\delta\theta(0)} \Big|_{\theta=0}. \quad (\text{A26})$$

Performing the  $U(1)_A$  rotation for quark fields together with flavor singlet condition [17], one can transfer the  $\theta$  dependence coupled to the topological gluon configurations, via the axial anomaly, to current quark mass terms. Thus  $\chi_{\text{top}}$  goes like [16]

$$\chi_{\text{top}} = \left( \frac{\langle \bar{u}u \rangle}{m_u} + \frac{\langle \bar{d}d \rangle}{m_d} + \frac{\langle \bar{s}s \rangle}{m_s} \right) \bar{m}^2 + \bar{m}^2 (\chi_P^{uu} + \chi_P^{dd} + 2\chi_P^{ud} + 2(\chi_P^{us} + \chi_P^{ds}) + \chi_P^{ss}), \quad (\text{A27})$$

where  $\chi_P^{uu,dd,ud}$ ,  $\chi_P^{ss}$  and  $\chi_P^{us,ds}$  are pseudoscalar susceptibilities in Eq.(A12) and  $\bar{m}$  is defined as

$$\bar{m} = \left( \frac{1}{m_u} + \frac{1}{m_d} + \frac{1}{m_s} \right)^{-1}. \quad (\text{A28})$$

Furthermore, using the Ward identities for the chiral  $SU(3)$  rotation [30], we can find the correlation between the quark condensate and the pseudoscalar susceptibilities, which are given as

$$\langle \bar{u}u \rangle + \langle \bar{d}d \rangle = -m_l (\chi_P^{uu} + \chi_P^{dd} + 2\chi_P^{ud}) + 2m_s (\chi_P^{us} + \chi_P^{ds}), \quad (\text{A29})$$

$$\langle \bar{s}s \rangle = -m_s \chi_P^{ss} + \frac{m_l}{2} (\chi_P^{us} + \chi_P^{ds}), \quad (\text{A30})$$

$$\langle \bar{u}u \rangle + \langle \bar{d}d \rangle = -m_l \chi_\pi, \quad (\text{A31})$$

Now, combining Eqs.(A29), (A30), and (A31), we find that the topological susceptibility in Eq.(A27) can be reduced to a disconnected part of a pseudoscalar susceptibility:

$$\begin{aligned} \chi_{\text{top}} &= \frac{1}{2} m_l m_s (\chi_P^{us} + \chi_P^{ds}) \\ &= \frac{1}{4} m_l^2 (\chi_P^{uu} + \chi_P^{dd} + 2\chi_P^{ud} - \chi_\pi) \\ &= m_l^2 \chi_{5,\text{disc}}. \end{aligned} \quad (\text{A32})$$

By rewriting Eq.(A32), we get our key equation which corresponds to Eq.(3) in the main text:

$$\chi_{\eta-\delta} = 4\chi_{5,\text{disc}} - \chi_{\delta-\pi}. \quad (\text{A33})$$

Equation (A33) is a very intriguing and helpful equation for us to see the relation between chiral symmetry and  $U(1)_A$  symmetry. The left hand side represents the tendency of the chiral restoration, while the right hand side is described by the topological susceptibility and the trend of  $U(1)_A$  restoration. This equation shows that the chiral restoration can be correlated with the  $U(1)_A$  restoration and the topological configuration of QCD. It has been argued in the literature (say, [42] and references therein) that that chiral and  $U(1)_A$  symmetry cannot simultaneously be restored. Now this discrepancy can be rephrased by Eq.(A33): it should be attributed to the topological configuration of QCD. In the chiral limit, since the topological configuration can be rotated away from QCD,  $\chi_{\text{top}}$  will come to be zero, which can also be seen directly from Eq.(A32). So the discrepancy will vanish and chiral symmetry and  $U(1)_A$  symmetry should be restored simultaneously.

#### Appendix B: Numerical calculation results

In this section, we give our numerical calculation results on the (subtracted) quark condensate, scalar and pseudoscalar susceptibilities, and topological susceptibility. We also check the consistency with the recent lattice QCD data on 2 + 1 flavors at physical point, and also with other chiral effective models,

## 1. Parameter setting

In the present model, in Eq.(A1), we have five parameters that need to be specified: the light quark mass  $m_l$ , the strange quark mass  $m_s$ , the coupling constants  $g_s$  and  $g_D$ , and the three-momentum cutoff  $\Lambda$ . To fix the parameters, we take the following four hadronic observables at  $T = 0$  as inputs:

$$m_\pi = 136 \text{ MeV}, \quad f_\pi = 93 \text{ MeV}, \quad m_K = 495.7 \text{ MeV}, \quad m_{\eta'} = 957.5 \text{ MeV}. \quad (\text{B1})$$

To fix the remaining one degree of freedom, we follow the literature [31] to take light quark mass  $m_l = 5.5 \text{ MeV}$  (at the renormalization scale of 1 GeV). Thus all the model parameters are fixed, which are presented in Table I [23].

TABLE I: Parameter setting

Parameters	Values
light quark mass $m_l$	5.5 MeV
strange quark mass $m_s$	138 MeV
four-fermion coupling constant $g_s$	0.358 fm <sup>2</sup>
six-fermion coupling constant $g_D$	- 0.0275 fm <sup>5</sup>
cutoff $\Lambda$	631.4 MeV

## 2. Subtracted quark condensate

The quark condensate in the NJL model involves a ultraviolet (UV) divergence (which is dominated by a quadratic divergence) due to its vacuum part ( $\langle -\bar{q}q \rangle \sim N_c m_q \Lambda^2 / (4\pi^2)$ ), and is needed to be renormalized when compared with lattice data. Since the quadratic divergences in the quark condensate come along with current quark masses (as above), we use a subtracted quark condensate as the chiral order parameter, which has been adopted in the lattice simulations:  $\Delta_{l,s}(T) \equiv \langle \bar{l}l \rangle - \frac{2m_l}{m_s} \langle \bar{s}s \rangle$ , where  $\langle \bar{l}l \rangle = \langle \bar{u}u \rangle = \langle \bar{d}d \rangle$ .

Figure 6 shows the subtracted quark condensate with respect to temperature predicted from the present NJL model, in comparison with the lattice QCD result on 2+1 flavor data at the physical point [32]. Note that in the figure, the temperature is normalized by the pseudo-critical temperature  $T_{pc}$ , which is (for the NJL prediction) defined as  $d^2 \langle \bar{l}l \rangle(T) / dT^2|_{T=T_{pc}}$ . We have found the  $T_{pc}|_{\text{NJL}} \simeq 188 \text{ MeV}$ , which is compared with the lattice result  $T_{pc}|_{\text{lat.}} \simeq 155 \text{ MeV}$  [33–37]. In the figure, we have thus normalized the temperature by their corresponding pseudo-critical temperature respectively.

From Fig. 6, we see that the subtracted quark condensate based on NJL calculation shows a perfect consistency with the lattice data. This confirms that the present NJL model describes the chiral crossover phenomenon quite well.

## 3. Chiral and axial susceptibility partners

The scalar and pseudoscalar susceptibilities presented in Eqs. (A14), (A16), (A23), and (A25) are correlated with each other by the chiral  $SU(3)_L \times SU(3)_R$  and  $U(1)_A$  transformations [38]:

$$\begin{array}{ccc}
 & \xleftrightarrow{SU(2)} & \\
 \chi_\pi & \longleftrightarrow & \chi_\sigma \\
 \uparrow U(1)_A & & \uparrow U(1)_A \\
 \chi_\delta & \longleftrightarrow & \chi_\eta \\
 & \xleftrightarrow{SU(2)} & 
 \end{array}$$

In the chiral-symmetry and  $U(1)_A$  symmetry-restoration limits, the corresponding partners will be equal to each other:

$$\chi_\pi = \chi_\sigma, \quad \chi_\delta = \chi_\eta \quad (\text{chiral symmetry limit}) \quad (\text{B2})$$

$$\chi_\pi = \chi_\delta, \quad \chi_\sigma = \chi_\eta \quad (\text{axial symmetry limit}) \quad (\text{B3})$$

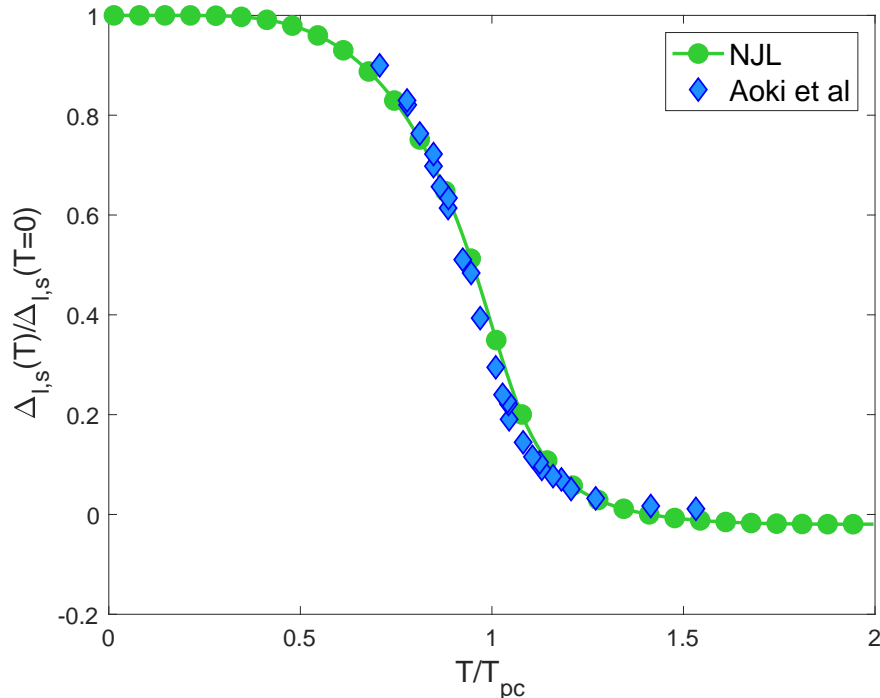


FIG. 6: Temperature scaling of the subtracted quark condensate, in comparison with data from the lattice QCD with 2 + 1 flavors [33]. The normalization factor, the pseudo-critical temperature for the chiral crossover ( $T_{pc}$ ) has been set to individual values estimated from the present NJL model ( $T_{pc|NJL} \simeq 188$  MeV) and the lattice simulation ( $T_{pc|lat.} \simeq 155$  MeV).

Then, observation of null difference between the above partners can effectively monitor the restoration of the related symmetry. Here we denote  $\chi_\pi - \chi_\delta$  as  $\chi_{\pi-\delta}$  and  $\chi_\eta - \chi_\delta$  as  $\chi_{\eta-\delta}$  to signal the  $U(1)_A$  symmetry and the chiral symmetry, respectively. To see exactly how the chiral symmetry and  $U(1)$  axial symmetry is restored with the increase of temperature, based on Eqs.(A14), (A16), and (A25), in Fig.7 we show our numerical result on the susceptibility differences as a function of temperature, in comparison to the lattice QCD result [11].

In Fig.7, we see that the chiral-partner difference  $\chi_{\eta-\delta}$  fits quite well with the lattice data, while the  $U(1)_A$ -partner difference  $\chi_{\pi-\delta}$  shows some discrepancy. Note that  $\chi_{\eta-\delta}$  and  $\chi_{\pi-\delta}$  are both normalized by  $T^2$  in Fig.7. For the unnormalized ones, the present NJL model seems to yield larger values for both  $\chi_{\eta-\delta}$  and  $\chi_{\pi-\delta}$  than what the lattice simulation currently predicts. We can still see the discrepancy between chiral and  $U(1)_A$  symmetry restorations. Both the NJL analysis and the lattice simulation predict a faster restoration of the chiral symmetry than the  $U(1)$  axial symmetry. This can also be seen from Eq.(A33), as it was discussed before. Since the topological susceptibility  $\chi_{top}$  keeps negative value in any temperature (due to the dominance of the quark condensate terms which are all negative), Eq.(A33) would indicate that  $\chi_{\eta-\delta}$  is always smaller than  $\chi_{\pi-\delta}$ . This trend holds for both the lattice and NJL results. We have further confirmed the faster restoration of the chiral symmetry at high temperature. Above the critical temperature  $T_{pc|NJL} \simeq 188$  MeV, we see a good enough approximate chiral symmetry from Fig.7. The effective- $U(1)_A$  restoration-temperature is estimated to be larger than 250 MeV.

#### 4. Topological susceptibility

The generic formula of topological susceptibility is given by Eq.(A27), which is composed of the quark condensate part and the pseudoscalar susceptibility part. Using the explicit formulas for the quark condensate in Eq.(A4) and the pseudooscalar susceptibility in Eq.(A12), we are ready to evaluate  $\chi_{top}$  with respect to temperature.

In Fig. 8, we plot the temperature dependence of unnormalized topological susceptibility  $\chi_{top}^{1/4}$ . We have found  $\chi_{top}$  keeps negative at any temperature, and taken the absolute value of  $\chi_{top}$  in the figure. Comparison with the dilute instanton gas approximation (DIGA) [25, 26], the linear sigma model result (denoted as CJT in the figure) [16] and the result from lattice simulation in the continuum limit [39–41] have also been displayed. The temperature is normalized by the pseudo-critical temperature in the figure. We have taken  $T_{pc|NJL} = 188$  MeV for the NJL case,

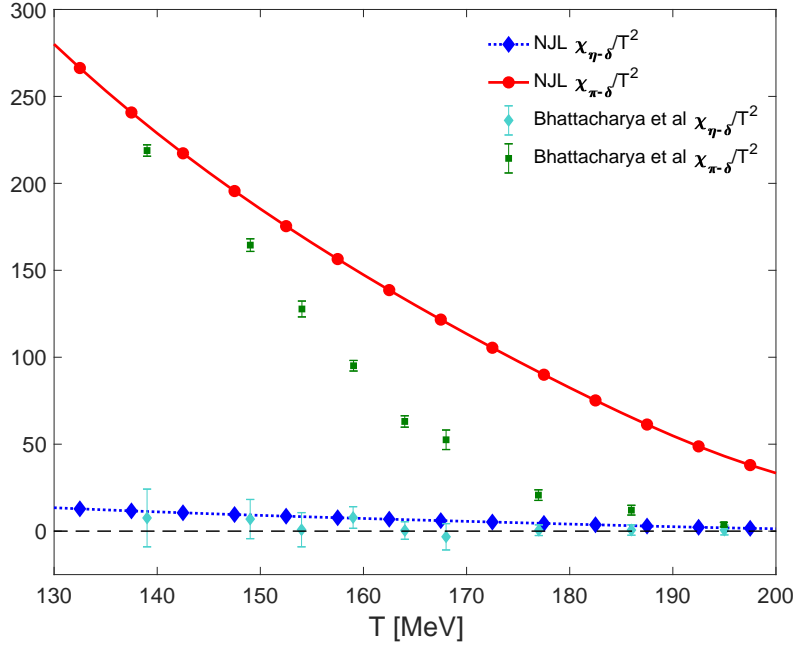


FIG. 7: Temperature dependence of the susceptibility differences around the chiral crossover, in comparison with lattice QCD data for 2 + 1 flavors [11].

$T_{pc|CJT} = 215$  MeV for the linear sigma model case, and  $T_{pc|lat} = 155$  MeV for the lattice and DIGA cases.

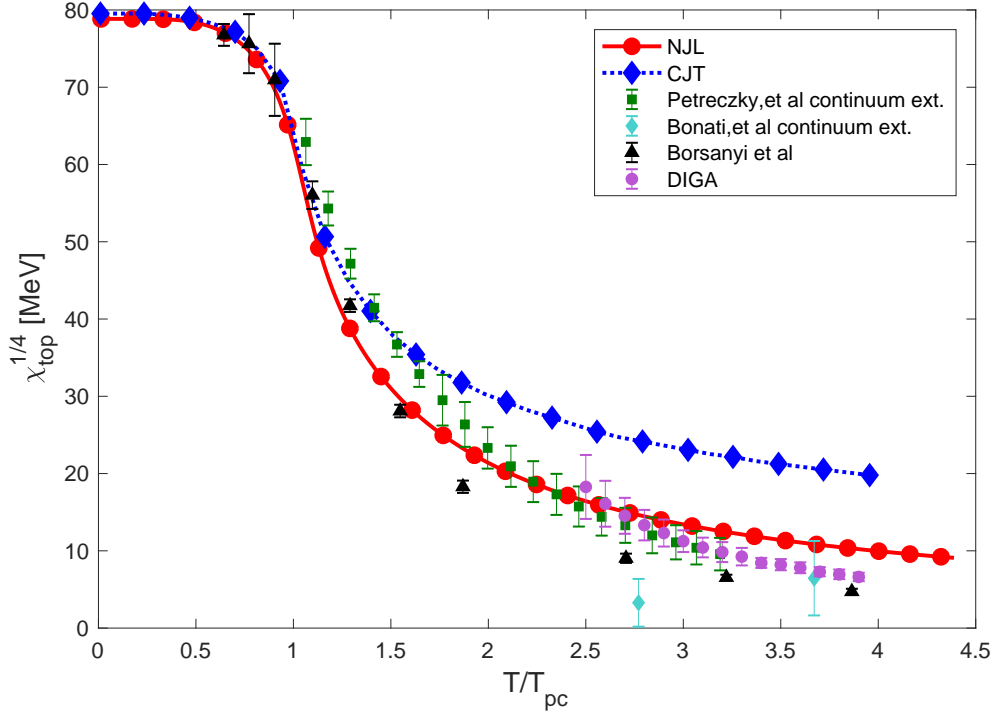


FIG. 8: Temperature scaling of topological susceptibilities, compared with lattice data [39–41] and other models as described in the text. The DIGA prediction has been quoted from the literature [39]. For the way of error bars associated with the DIGA, see the cited reference.

Figure 8 shows perfect consistency between the NJL analysis and lattice result. We see they maintain a good agreement with each other in the whole range of the available lattice data,  $T/T_{pc} \sim 0 - 4$ . Below the pseudo-critical temperature,  $T < T_{pc}$ , all the results fit perfectly with each other, including the linear sigma model. In contrast, as temperature goes higher than the pseudo-critical temperature,  $T > T_{pc}$ , we see the deviation of linear sigma model from the NJL and lattice results. In the literature [16], their analysis on the linear sigma model the pseudoscalar susceptibility part was not able to evaluate, because the authors did not include the higher order terms in the current quark mass matrix, and therefore performing the second order derivative on the mass parameter to obtain pseudoscalar susceptibility would not work out. Thus, their  $\chi_{top}$  only includes the quark condensate part. The present NJL model is able to give the pseudoscalar susceptibility contribution to  $\chi_{top}$ , to achieve an improved estimate on the quark condensate, and therefore the figure shows better consistency with the lattice result.

### Appendix C: A conjectured high T-QCD model

To evaluate the trilemma-relaxation estimator  $R$  for a higher  $T$  like  $T > 300$  MeV, we may consider a quarkonic-interacting model in a sense of quantum field theory, instead of dilute instanton gas by which it would be hard to compute thermally-averaged Green functions like  $R$ . We shall approximate such an interacting quark gas at high  $T$  (say, quark-gluon plasma) by only the kinetic and determinant terms which would play a role of the gluonic counterpart acting as if it is like a dilute instanton effect among quarks. The size of the determinant coupling should be small, so that the chiral symmetry is broken only by the current quark masses: the coupling should not exceed the critical value. In addition, as the temperature gets higher, the QCD instanton effect should be suppressed by a Boltzmann-like factor as predicted from the dilute instanton gas description [25, 26], so that in terms of quarkonic interactions the determinant term would be suppressed as well.

Thus we write a conjectured model for high- $T$  QCD with three quark flavors as

$$\mathcal{L}_{\text{high-T}} = \bar{q}(i\gamma_\mu\partial^\mu - \mathbf{m})q + K(T)[\det(\bar{q}_L q_R) + \text{h.c.}], \quad (\text{C1})$$

where  $K(T)$  is the temperature-dependent coupling strength of the determinant term, which simply models the Boltzmann-like suppression for the QCD instanton configuration:  $K(T) = e^{-T^2/\mu_{\text{QCD}}^2} K$ , with a collective scale factor of QCD,  $\mu_{\text{QCD}}^2$  and the overall constant  $K$  being scaled by the model cutoff  $\Lambda$  along with a dimensionless parameter  $k$  like  $K = k/\Lambda^2$ .

For a benchmark evaluation of  $R$ , we set the parameters as

$$\mu_{\text{QCD}} = 200, 300, 400 \text{ MeV}, \quad \Lambda = 3 \text{ GeV}, \quad k = -0.5. \quad (\text{C2})$$

where the parameter  $k$  has been chosen so as not to exceed the critical coupling  $k_{\text{cr}} = -\pi^2/3$ . With the parameter setting above, this model can work for  $T \sim 300$  MeV up to the order of  $O(1 \text{ GeV})$ .

To calculate all the quantities relevant to  $R$ , we only need to refer to the NJL model case, just by replacing  $g_D$  with  $K(T)$  and setting the four-fermion coupling strength  $g_s = 0$ . The plots of  $R$  are thus given in Fig.5 in the main text.

- [1] M. Shaposhnikov, [arXiv:0708.3550 [hep-th]].
- [2] H. B. Nielsen, Bled Workshops Phys. **13**, no.2, 94-126 (2012) [arXiv:1212.5716 [hep-ph]].
- [3] I. Masina, Phys. Rev. D **87**, no.5, 053001 (2013) doi:10.1103/PhysRevD.87.053001 [arXiv:1209.0393 [hep-ph]].
- [4] G. Degrossi, S. Di Vita, J. Elias-Miro, J. R. Espinosa, G. F. Giudice, G. Isidori and A. Strumia, JHEP **08**, 098 (2012) doi:10.1007/JHEP08(2012)098 [arXiv:1205.6497 [hep-ph]].
- [5] R. D. Peccei and H. R. Quinn, Phys. Rev. D **16** (1977), 1791-1797 doi:10.1103/PhysRevD.16.1791
- [6] M. A. Shifman, A. I. Vainshtein and V. I. Zakharov, Nucl. Phys. B **166** (1980), 493-506 doi:10.1016/0550-3213(80)90209-6
- [7] J. E. Kim and G. Carosi, Rev. Mod. Phys. **82** (2010), 557-602 [erratum: Rev. Mod. Phys. **91** (2019) no.4, 049902] doi:10.1103/RevModPhys.82.557 [arXiv:0807.3125 [hep-ph]].
- [8] S. Weinberg, [arXiv:astro-ph/0005265 [astro-ph]].
- [9] S. Weinberg, Phys. Rev. Lett. **40** (1978), 223-226 doi:10.1103/PhysRevLett.40.223
- [10] F. Wilczek, Phys. Rev. Lett. **40** (1978), 279-282 doi:10.1103/PhysRevLett.40.279
- [11] T. Bhattacharya, M. I. Buchoff, N. H. Christ, H. T. Ding, R. Gupta, C. Jung, F. Karsch, Z. Lin, R. D. Mawhinney and G. McGlynn, *et al.* Phys. Rev. Lett. **113**, no.8, 082001 (2014) doi:10.1103/PhysRevLett.113.082001 [arXiv:1402.5175 [hep-lat]].
- [12] S. Aoki, H. Fukaya and Y. Taniguchi, Phys. Rev.

- D **86**, 114512 (2012) doi:10.1103/PhysRevD.86.114512 [arXiv:1209.2061 [hep-lat]].
- [13] T. D. Cohen, Phys. Rev. D **54**, R1867-R1870 (1996) doi:10.1103/PhysRevD.54.R1867 [arXiv:hep-ph/9601216 [hep-ph]].
- [14] T. D. Cohen, [arXiv:nucl-th/9801061 [nucl-th]].
- [15] S. Aoki *et al.* [JLQCD], [arXiv:2103.05954 [hep-lat]].
- [16] M. Kawaguchi, S. Matsuzaki and A. Tomiya, Phys. Rev. D **103**, no.5, 054034 (2021) doi:10.1103/PhysRevD.103.054034 [arXiv:2005.07003 [hep-ph]].
- [17] V. Baluni, Phys. Rev. D **19**, 2227-2230 (1979) doi:10.1103/PhysRevD.19.2227
- [18] M. Kawaguchi, S. Matsuzaki and A. Tomiya, Phys. Lett. B **813**, 136044 (2021) doi:10.1016/j.physletb.2020.136044 [arXiv:2003.11375 [hep-ph]].
- [19] M. Kobayashi and T. Maskawa, Prog. Theor. Phys. **44**, 1422-1424 (1970) doi:10.1143/PTP.44.1422
- [20] M. Kobayashi, H. Kondo and T. Maskawa, Prog. Theor. Phys. **45**, 1955-1959 (1971) doi:10.1143/PTP.45.1955
- [21] G. 't Hooft, Phys. Rev. Lett. **37**, 8-11 (1976) doi:10.1103/PhysRevLett.37.8
- [22] G. 't Hooft, Phys. Rev. D **14**, 3432-3450 (1976) [erratum: Phys. Rev. D **18**, 2199 (1978)] doi:10.1103/PhysRevD.14.3432
- [23] T. Hatsuda and T. Kunihiro, Phys. Rept. **247**, 221-367 (1994) doi:10.1016/0370-1573(94)90022-1 [arXiv:hep-ph/9401310 [hep-ph]].
- [24] R. D. Pisarski and F. Rennecke, Phys. Rev. D **101**, no.11, 114019 (2020) doi:10.1103/PhysRevD.101.114019 [arXiv:1910.14052 [hep-ph]].
- [25] R. D. Pisarski and L. G. Yaffe, Phys. Lett. B **97**, 110-112 (1980) doi:10.1016/0370-2693(80)90559-6
- [26] D. J. Gross, R. D. Pisarski and L. G. Yaffe, Rev. Mod. Phys. **53**, 43 (1981) doi:10.1103/RevModPhys.53.43
- [27] S. Iso, P. D. Serpico and K. Shimada, Phys. Rev. Lett. **119**, no.14, 141301 (2017) doi:10.1103/PhysRevLett.119.141301 [arXiv:1704.04955 [hep-ph]].
- [28] T. Kunihiro, Nucl. Phys. B **351** (1991), 593-622 doi:10.1016/S0550-3213(05)80035-5
- [29] A. Gomez Nicola and J. Ruiz de Elvira, Phys. Rev. D **97** (2018) no.7, 074016 doi:10.1103/PhysRevD.97.074016 [arXiv:1704.05036 [hep-ph]].
- [30] A. Gómez Nicola and J. Ruiz de Elvira, JHEP **03** (2016), 186 doi:10.1007/JHEP03(2016)186 [arXiv:1602.01476 [hep-ph]].
- [31] G. A. Miller, B. M. K. Nefkens and I. Slaus, Phys. Rept. **194** (1990), 1-116 doi:10.1016/0370-1573(90)90102-8
- [32] Y. Aoki, S. Borsanyi, S. Durr, Z. Fodor, S. D. Katz, S. Krieg and K. K. Szabo, JHEP **06** (2009), 088 doi:10.1088/1126-6708/2009/06/088 [arXiv:0903.4155 [hep-lat]].
- [33] Y. Aoki, G. Endrodi, Z. Fodor, S. D. Katz and K. K. Szabo, Nature **443** (2006), 675-678 doi:10.1038/nature05120 [arXiv:hep-lat/0611014 [hep-lat]].
- [34] S. Borsanyi *et al.* [Wuppertal-Budapest], J. Phys. Conf. Ser. **316** (2011), 012020 doi:10.1088/1742-6596/316/1/012020 [arXiv:1109.5032 [hep-lat]].
- [35] H. T. Ding, F. Karsch and S. Mukherjee, Int. J. Mod. Phys. E **24** (2015) no.10, 1530007 doi:10.1142/S0218301315300076 [arXiv:1504.05274 [hep-lat]].
- [36] A. Bazavov *et al.* [HotQCD], Phys. Lett. B **795** (2019), 15-21 doi:10.1016/j.physletb.2019.05.013 [arXiv:1812.08235 [hep-lat]].
- [37] H. T. Ding, Nucl. Phys. A **1005** (2021), 121940 doi:10.1016/j.nuclphysa.2020.121940 [arXiv:2002.11957 [hep-lat]].
- [38] A. Bazavov *et al.* [HotQCD], Phys. Rev. D **86** (2012), 094503 doi:10.1103/PhysRevD.86.094503 [arXiv:1205.3535 [hep-lat]].
- [39] P. Petreczky, H. P. Schadler and S. Sharma, Phys. Lett. B **762** (2016), 498-505 doi:10.1016/j.physletb.2016.09.063 [arXiv:1606.03145 [hep-lat]].
- [40] C. Bonati, M. D'Elia, M. Mariti, G. Martinelli, M. Mesiti, F. Negro, F. Sanfilippo and G. Villadoro, JHEP **03** (2016), 155 doi:10.1007/JHEP03(2016)155 [arXiv:1512.06746 [hep-lat]].
- [41] S. Borsanyi, Z. Fodor, J. Guenther, K. H. Kampert, S. D. Katz, T. Kawanai, T. G. Kovacs, S. W. Mages, A. Pasztor and F. Pittler, *et al.* Nature **539** (2016) no.7627, 69-71 doi:10.1038/nature20115 [arXiv:1606.07494 [hep-lat]].
- [42] H. T. Ding, S. T. Li, S. Mukherjee, A. Tomiya, X. D. Wang and Y. Zhang, Phys. Rev. Lett. **126**, no.8, 082001 (2021) doi:10.1103/PhysRevLett.126.082001 [arXiv:2010.14836 [hep-lat]].